Chinese Journal of Polymer Science Vol. 31, No. 5, (2013), 778−786

Chinese Journal of Polymer Science
© Chinese Chemical Society
Institute of Chemistry, CAS
Springer-Verlag Berlin Heidelberg 2013

DOXORUBICIN-LOADED BORON-RICH POLYMER NANOPARTICLES FOR ORTHOTOPICALLY IMPLANTED LIVER TUMOR TREATMENT*

Lu-zhong Zhang[a, b], Ya-jun Zhang[a], Wei Wu[a**] and Xi-qun Jiang[a**]

[a] *Laboratory of Mesoscopic Chemistry and Department of Polymer Science & Engineering, College of Chemistry & Chemical Engineering; Jiangsu Provincial Laboratory for Nanotechnology, Nanjing University, Nanjing 210093, China*

[b] *Jiangsu Key Laboratory of Neuroregeneration, Nantong University, Nantong 226001, China*

Abstract The *in vivo* behaviors of doxorubicin (DOX)-loaded dextran-poly(3-acrylamidophenylboronic acid) (Dextran-PAPBA) nanoparticles (NPs) were studied. The DOX-loaded NPs had a narrowly distributed diameter of *ca.* 74 nm and mainly accumulated in liver of tumor-bearing mice after intravenous injection as demonstrated by *in vivo* real-time near infrared fluorescent imaging. The DOX contents in various tissues were quantified and consisted well with the results of fluorescent imaging. The biodistribution pattern of DOX-loaded NPs encourages us to investigate their liver tumor treatment by using an orthotopically implanted liver tumor model, revealing that the DOX-loaded NPs formulation had better antitumor effect than free DOX.

Keywords: Dextran-PAPBA nanoparticles; DOX; Drug delivery; Antitumor.

INTRODUCTION

Chemotherapy has been considered to be an important and effective therapeutic mean for the tumor treatment[1, 2]. However, most antitumor agents inherently exhibit serious side effects and inability to achieve satisfactory therapeutic efficiency that bring great pains the patients[3, 4]. Accordingly, it is extremely pressing to seek new effective pharmacological formulations for the tumor treatment. Nano drug delivery systems (NDDS) have shown great potentials in their capacities to overcome these existing clinical problems[5, 6] and exhibited significant advantages over conventional therapeutic agents, such as effective protection of the drugs, prolonged circulation in the bloodstream, enhanced permeation and retention (EPR) effect in tumor, low side effects, *etc*[7–9].

When designing NDDS, one need to comprehensively consider various physicochemical properties of NDDS and their components, including biocompatibility, degradability, size, shape and surface chemistry, *etc*[10]. These factors determine jointly their performance as drug carriers. Polymeric nanoparticles (NPs) are one sort of attractive drug carriers and have been extensively studied due to their significant superiority in biocompatibility, biodegradation and tenability[11, 12]. Up to now, various synthetic and natural polymers have been used to fabricate NPs for drug delivery[13–18]. The fabricate methods involve the assembly of amphiphilic di- or tri-block copolymers or partially hydrophobically modified natural polymers in aqueous medium and the assembly of oppositively charged polyelectrolytes, *etc*[19, 20].

* This work was financially supported by the National Natural Science Foundation of China (Nos. 51033002 and 51273090).
** Corresponding authors: Wei Wu (武伟), E-mail: wuwei@nju.edu.cn
Xi-qun Jiang (蒋锡群), E-mail: jiangx@nju.edu.cn
Invited paper dedicated to Professor Fosong Wang on the occasion of his 80th birthday
Received December 19, 2012; Revised January 10, 2013; Accepted January 21, 2013
doi: 10.1007/s10118-013-1267-y

In our previous work, we have reported a simple method to prepare dextran-containing NPs by polymerizing 3-acrylamidophenylboronic acid (APBA) monomer in aqueous solution of dextran, and the synthesized NPs were named Dextran-PAPBA NPs. In this system, dextran interacts with boronic groups *via* a reversible boronic acid-diol reaction, which has been demonstrated and monitored by ^{11}B-NMR. The NPs are stable over a wide range of pH and temperature and have narrowly distributed size. The size and composition of the NPs can be easily regulated by changing the feeding ratio of dextran to APBA. Herein, we present the studies of the *in vivo* behaviors of the DOX-loaded Dextran-PAPBA NPs and their antitumor performance on an orthotopic hepatic tumor model. The results demonstrate that the doxorubicin (DOX)-loaded NPs had significantly superior efficacy in impeding tumor growth than free DOX.

EXPERIMENTAL

Materials and Methods

Dextran was bought from Pharmacia Company (M_w, *ca*. 3000). 4,4′-Azobis(4-cyanovaleric acid) was obtained from Acros Organics Company. Doxorubicin (DOX) hydrochloride was purchased from Shanghai Aladdin Reagent Company. 3-Acrylamidophenylboronic acid was synthesized following published procedures[21]. NIR-797 was purchased from Aldrich. Gadopentetate Dimeglumine Injection (Gd-DTPA) was purchased from Beijing Beilu Pharmaceutical (Beijing, China). The morphology of DOX loaded NPs was observed by transmission electron microscopy (TEM, JEOL-100).

Preparation of Dextran-PAPBA NPs

Dextran-PAPBA NPs was prepared following our published procedures[22]. Briefly, 152 mg of dextran and 90 mg of 3-acrylamidophenylboronic acid were dissolved in 12 mL of water by heating. Thereafter, 9.4 mg of 4,4′-azobis(4-cyanovaleric acid) was added, and the pH value of the resulting solution was adjusted to *ca*. 6.3 with sodium hydroxide solution. The resulting mixture was stirred at 80 °C. When the reaction mixture became opalescent, the reaction was allowed to proceed for another 2 h. The prepared NPs were purified by dialysis against 1 L of deionized water in a 100 kDa MWCO membrane for 10 h and collected after lyophilization.

Preparation of DOX-loaded Dextran-PAPBA NPs

To a stirred suspension of Dextran-PAPBA NPs in water (5 mg/mL, 5 mL), of which the pH was adjusted to 8.2 with sodium hydroxide solution beforehand, a DOX aqueous solution (3 mg/mL, 1 mL) was added. The resulting mixture was stirred for 12 h. Thereafter, the mixture was centrifuged at 10000 r/min for 30 min to remove free DOX. The precipitation was redispersed in predetermined volume of glucose injection, giving a suspension of DOX-loaded Dextran-PAPBA NPs. The drug loading content and encapsulation efficiency were determined following published procedures[22].

Preparation of Near Infrared (NIR) Dye-labeled DOX-loaded Dextran-PAPBA NPs

To a suspension of DOX-loaded Dextran-PAPBA NPs in water (5 mg/mL, 5 mL), of which the pH was adjusted to 8.0 with sodium hydroxide beforehand, was added 4 mg of NIR-797. The resulting solution was stirred at room temperature under dark for 24 h. Thereafter, the resulting solution was dialyzed against 1 L of deionized water for 24 h in a 10 kDa MWCO membrane to remove excess free NIR-797. The mixture was centrifuged at 10000 r/min for 30 min and the precipitation was redispersed in predetermined volume of glucose injection, giving a suspension of NIR-797-labeled DOX-loaded Dextran-PAPBA NPs.

In vivo Real-time Imaging

All animal experiments were performed in accordance with the guidelines for animal experiments and are approved by the Animal Care Committee at Drum Tower Hospital. To establish the experimental tumor model, the murine hepatic H22 tumor cells (5×10^6–6×10^6 cells per mouse) were inoculated subcutaneously into the armpit of male ICR mice (6–8 weeks, provided by Central Animal Laboratory of Nanjing Medical University). Tumor growth was monitored until an acceptable size. The NIR-797-labeled DOX-loaded NPs were then injected *via* tail vein at a dose of 5 mg of DOX equivalent (equiv.) per kilogram of body weight in 0.3 mL of

glucose injection. Three mice were used in this study. The mice were anesthetized with isoflurane at various time points post-injection and imaged using the Maestro *in vivo* optical imaging system (CRi, Inc., Woburn, MA). At the completion of the *in vivo* imaging, the mice were sacrificed and the tumor, heart, liver, spleen, lung, kidney, brain, intestine and stomach were harvested for isolated organ imaging.

DOX Distribution in Tumor-bearing Mice

The tumor models were established as mentioned above. The tumor-bearing mice were randomly assigned to two groups and injected respectively free DOX and DOX-loaded NPs at a dose of 5 mg of DOX equiv. per kilogram of body weight in 0.3 mL of glucose injection *via* tail vein. The mice (23–30 g) were sacrificed at 1, 3, 6, 12, 24, 48 h post injection ($n = 3$ for each time point). Subsequently, the tumor, liver, spleen, kidney, lung and heart were excised, and blood was collected, heparinized and centrifuged to obtain the plasma. The DOX concentrations in the organs and plasma were measured based on a method reported by Bae group[23]. The samples were suspended in 70% ethanol with 0.3 mol/L HCl and then homogenized to extract DOX. After centrifugation, the amount of DOX in the supernatant was determined by measuring the fluorescence at 590 nm (Shimadzu, RF-5301PC, Japan) and using a pre-established calibration curve.

Orthotopic Implantation of H22 Cells

The mice were anesthetized with an intraperitoneal injection of diazepatn and katamine hydrochloride before surgery. Their abdomens were made sterilized with 0.2% iodine tincture. The anesthetized mouse was laid on its back, and a 1 cm transverse incision was made through the skin and peritoneum of the left upper abdomen. H22 tumor cells (2.5×10^6 cells per mouse) in a 10 μL volume were injected into the subsera of the liver by using a 25 μL syringe. After swabbing the area with sterile gauze, the peritoneum was closed with 4–0 absorbable suture, and the skin was closed with wound clips. After the implantation, the orthotopic H22 tumor rapidly developed in the liver and was monitored by magnetic resonance imaging (MRI) on 7 days. Animals were randomized into different groups with eight animals in each group: Saline, blank Dextan-PAPBA NPs, free DOX, DOX loaded Dextan-PAPBA NPs. Each DOX formulation was injected *via* tail vein at a dose of 5 mg/kg DOX equiv. in 0.3 mL of glucose injection twice at 7-day intervals (day 0 and 7). On day 0 and 14, the mice were administrated intravenously with Gd-DTPA at a dose of 0.3 mg/kg, and anesthetized with isoflurane. Then, the animals were imaged using the MRI system (Bruker PharmaScan 7T) after 15 min post-injection of MRI agents.

Histology Observation

The tumor tissues from the groups treated with DOX-loaded NPs, blank Dextran-PAPBA NPs, free DOX and saline were dissected and fixed in 10% neutral buffered formalin. The tissues were processed routinely to paraffin, sectioned at 4 μm, stained with hematoxylin and eosin (H & E) and examined by optical microscopy.

RESULTS AND DISCUSSION

Preparation of DOX-loaded Dextran-PAPBA NPs

In our previous work, we have demonstrated that Dextran-PAPBA NPs can be readily prepared by polymerizing the monomer of APBA in an aqueous solution of dextran that interacts with APBA *via* a boronic acid-diol reaction[22]. DOX can be encapsulated into the NPs with a loading of 10% and encapsulation efficiency of 98% and exhibits a sustained and strongly pH-dependent release profile. Figure 1 shows a typical transmission electron microscopy (TEM) image of the DOX-loaded Dextran-PAPBA NPs. It can be observed that the NPs have a spherical shape with a narrowly distributed diameter of *ca*. 74 nm, which is slightly larger than that of the blank NPs.

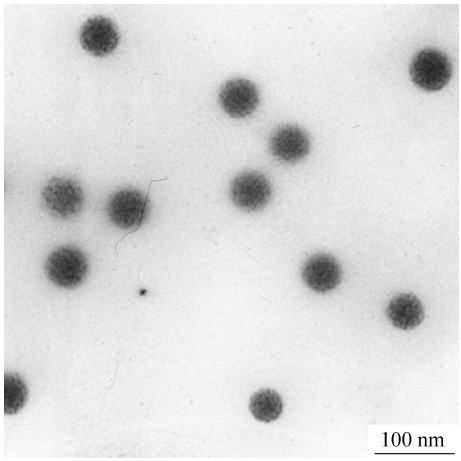


Fig. 1 Typical TEM image of DOX-loaded Dextran-PAPBA NPs
The feeding molar ratio of glucopyranoside unit in dextran to APBA is 2:1 in preparation.

In vivo Imaging of the Mice Injected NIR Dye-labeled DOX-Loaded Dextran-PAPBA NPs

As a prelude of the *in vivo* examinations of the NPs discussed below in this section, we have published the *in vitro* cytotoxicity of the DOX-loaded Dextran-PAPBA NPs with free DOX as a positive control, revealing that at low DOX concentrations (0.5–4 μg/mL), the DOX-loaded NPs exhibit lower cytotoxicity than free DOX and at a higher concentration (8 μg/mL), they have a comparable cytotoxicity[22]. To evaluate the fate of the DOX-loaded NPs in living body, we studied the biodistributions of the DOX-loaded NPs in tumor-bearing mice by using real time NIR fluorescence imaging after injecting the labeled NPs *via* tail vein[24]. The *in vivo* model animal was subcutaneous hepatic H22 transplanted tumor bearing mice. The DOX-loaded Dextran-PAPBA NPs were labeled by an NIR dye (NIR-797) through the reaction of isothiocyanate group on the dye with the hydroxyl groups on the NPs. Figure 2 shows the time-dependent NIR fluorescence images of a tumor-bearing mouse after injecting the labeled NPs *via* tail vein. An interesting observation is that the dominant fluorescence signal is viewed in liver from 1 h to 24 h post injection and no fluorescence signal can be observed in the region of tumor. At 48 h post injection, besides the liver region, signals can also be observed in the region of stomach. To confirm the distribution of the NPs, the different organs including heart, liver, spleen, lung, kidney, stomach, brain, intestine and tumor were excised at the completion of the 48 h *in vivo* imaging and imaged (Fig. 3). It is found that the fluorescence signals can be observed in the liver, stomach, spleen and intestine. Based on the results of the NIR fluorescence imaging, it can be essentially speculated that the Dextran-PAPBA NPs are mainly distributed in liver after intravenous injection and excreted *via* the hepatobiliary transport and end up in feces[25, 26].

Quantitative Analysis of the DOX Distribution

To precisely understand the drug delivery performance of the Dextran-PAPBA NPs in living body, we tested the DOX content in various tissues of tumor-bearing mice after injecting the DOX-loaded Dextran-PAPBA NPs with free DOX as control. Figure 4 shows the DOX concentrations in plasma at various time points after administration of free DOX injection and DOX-loaded NPs at a dose of 5 mg/kg DOX equiv. For DOX-loaded NPs, at 1 h post injection, the concentration of DOX in plasma is *ca*. 15.20 μg/g and decreases to *ca*. 0.73 μg/g at 48 h post injection. In contrast, in the case of the free DOX, DOX concentration in plasma is *ca*. 8.27 μg/g at 1 h post injection and rapidly decreases to *ca*. 0.14 μg/g at 48 h post injection. The DOX concentration profiles in plasma indicate that the encapsulation of DOX by Dextran-PAPBA NPs can prolong the blood circulation time of DOX and thus may be favorable to the tumor accumulation of DOX *via* the EPR effect of the NPs.

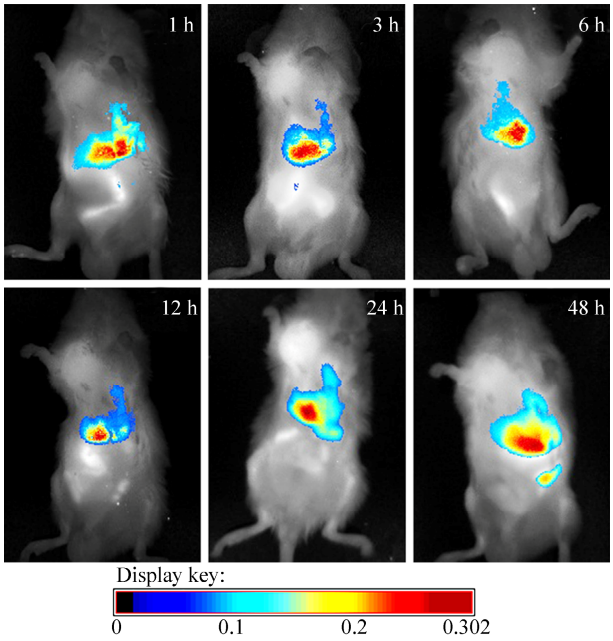


Fig. 2 *In vivo* fluorescence imaging of tumor-bearing mice after intravenous injection of the NPs

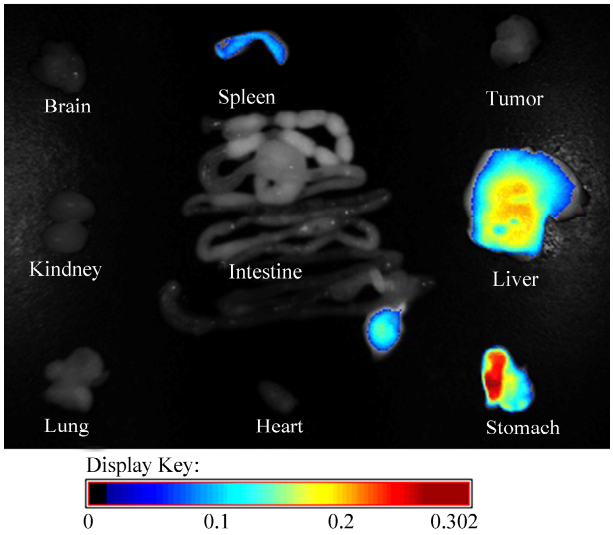


Fig. 3 The fluorescence image of various organs 48 h after intravenous injection

The distribution patterns of DOX in the other tissues are displayed in Fig. 5. In the case of the DOX-loaded NP formulation (Fig. 5a), it can be seen that among all the tested tissues, liver has the highest drug content. The DOX concentration in liver is *ca*. 30.95 μg/g at 1 h post injection and decrease to *ca*. 11.84 μg/g at 48 h post injection. Whereas, for the free DOX treated mice, the DOX concentration in liver is relatively low and decays faster. For example, the DOX concentration in liver is *ca*. 17.59 μg/g at 1 h post injection and decreases sharply to *ca*. 0.11 μg/g at 48 h post injection. For the DOX-loaded NPs, the longer retention time of DOX in liver may be associated with the covalent interaction between the lipid- and protein-bound sialic acid in liver and poly(*N*-3-acrylamidophenylboronic acid) in the NPs, since there is diol group in the molecule of sialic acid that can react with the boronic acid group in NPs[27, 28]. Comparing to the case of free DOX, there is smaller amount of DOX in heart in the case of DOX-loaded NPs, which is helpful to relieve the inherent cardiac side effect of DOX[29, 30]. In addition, it is worth noting that much less DOX is detected in the tumor of the mice treated by DOX-loaded NPs

than those treated by free DOX, which is well consistent with the results of fluorescence imaging. Although the concrete reason is not clear for the moment, this distribution pattern of the DOX-loaded Dextran-PAPBA NPs in tumor-bearing mice encourages us to study their antitumor performance on orthotopically implanted liver tumor, since the high content and long retention time in liver.

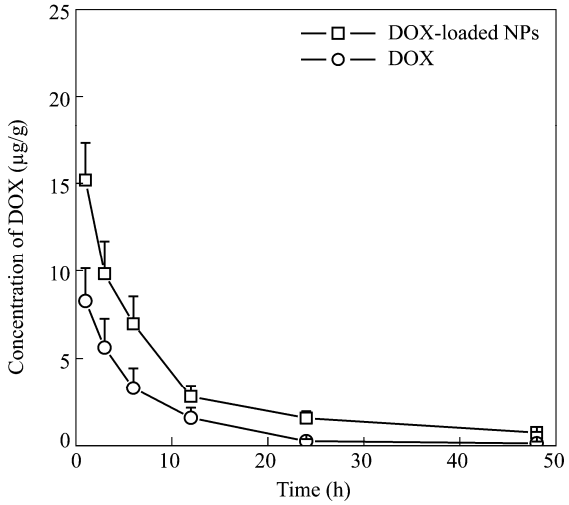


Fig. 4 The DOX concentrations in plasma of mice over 48 h after injection

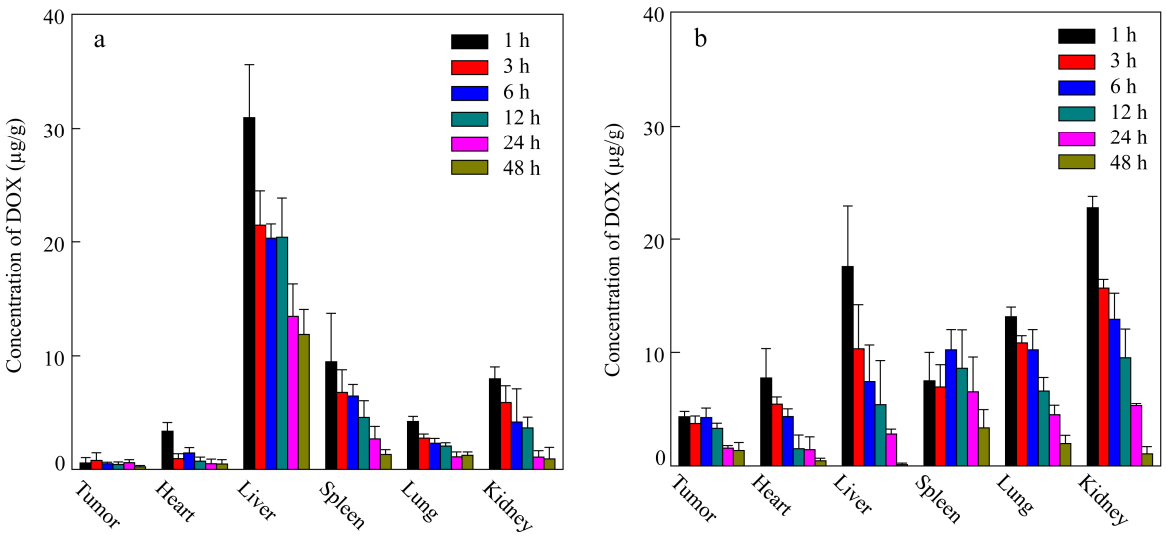


Fig. 5 Biodistribution of DOX in different organs of hepatic H22 tumor-bearing mice at various time points after a dose of 5 mg/kg through tail vein injection with DOX loaded NPs (a) and free DOX (b)

***In vivo* Antitumor Effect of the DOX-loaded NPs**

To examine whether the high content and long retention time of the DOX-loaded NPs in liver is benefit to liver tumor treatment, we studied their antitumor performance by using the mice with orthotopically implanted murine hepatic tumor as animal model and free DOX as a positive control. Both of the two DOX formulations were injected *via* tail vein at a dose of 5 mg/kg DOX equiv. twice at 7-day intervals. Blank NPs and saline were used as negative controls. After the treatments, the tumor volumes of the animals were examined by MRI. Figure 6 shows the variation of the tumor volume before and after the treatments with saline, blank NPs, free DOX and DOX-loaded NPs, respectively. The H22 tumors were located in hepatic parenchyma, and there was a clear demarcation between the tumor and the non-tumor region. Both groups treated respectively with saline and blank

NPs display rapid tumor growth in the 14 days after administration. In contrast, significant antitumor effect of the free DOX and DOX loaded NPs was observed. On the 14th day after administration, the tumor volumes of the group treated with the DOX-loaded NPs are obviously smaller than those of the group treated with free DOX. The gross images also demonstrate the same results (Fig. 6). Figure 7 shows the survival curves of the tumor-bearing mice. All of the mice treated with saline and blank NPs died within 16 days after treatments and only one animal survived for the group treated with free DOX. In contrast, four of the eight mice in the group treated with DOX-loaded NPs survived on the 16th day after treatment. It is further demonstrated that the DOX-loaded NPs have the better antitumor efficacy than the free DOX.

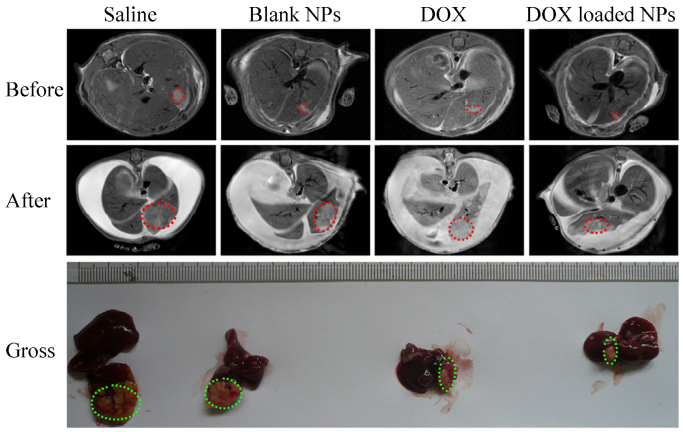


Fig. 6 Representive MR images, gross images of *in vivo* antitumor effects in mice model at dose of 10 mg/kg in ICR mice models (saline, blank NPs, DOX, DOX loaded NPs)

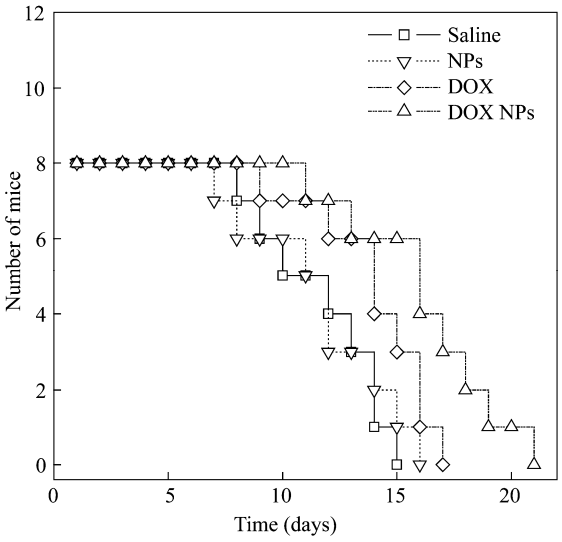


Fig. 7 Kaplan-Meier curves showing survival of tumor-bearing mice in each treated group

Histology Studies

To verify the necrosis level of the tumor tissue from the groups treated with saline, blank NPs, free DOX and DOX loaded NPs, the mice were sacrificed at the completion of tumor suppression study, and the tumors were resected. The tumor slices were stained by hematoxylin and eosin (H & E) and analyzed *via* the optical microscopy (Fig. 8). Large-area apoptotic or necrotic regions can be observed in the DOX-loaded NPs treated

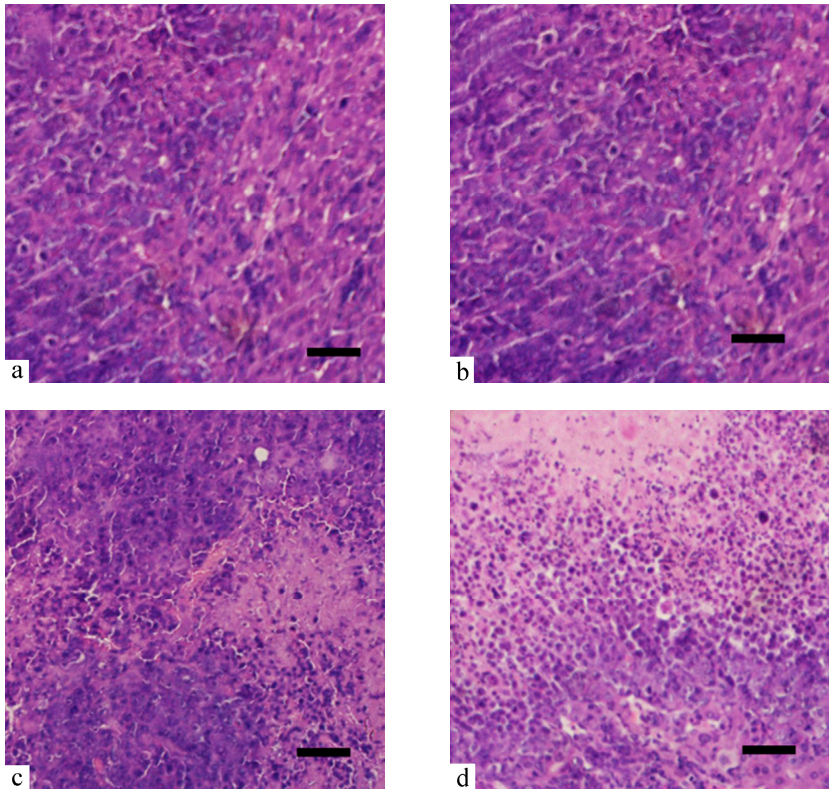


Fig. 8 H&E stained tumor slices from mice on the 15th day after treatments with saline (a), blank NPs (b), free DOX (c) and the DOX loaded NPs (d) (The scale bar represents 50 μm.)

tumor. In contrast, the free DOX treated tumors display a much lower apoptotic level with a large amount of living cells existing. The tumor treated with saline and blank NPs exhibited similar parallel and the lowest apoptotic region.

CONCLUSIONS

The *in vivo* behaviors of DOX-loaded Dextran-PAPBA NPs in tumor-bearing mice were investigated by NIR fluorescence imaging and quantitative analysis of DOX content in various tissues, revealing that these NPs were mainly distributed in the liver of tumor-bearing mice after intravenous injection. Although the reason of this phenomenon is not clear yet, the better antitumor effect of the DOX-loaded Dextran-PAPBA NPs on orthotopically implanted liver tumor than free DOX was demonstrated, which may be associated with the high content and long retention time of the NPs in liver.

REFERENCES

1 Fox, M.E., Szoka, F.C. and Frechet, J.M.J., Acc. Chem. Res., 2009, 42(8): 1141
2 Tian, Q., Zhang, C.N., Wang, X.H., Wang, W., Huang, W., Cha, R.T., Wang, C.H., Yuan, Z., Liu, M., Wan, H. and Tang, H., Biomaterials, 2010, 31(17): 4748
3 Ding, D., Zhu, Z.S., Liu, Q., Wang, J., Hu, Y., Jiang, X.Q. and Liu, B.R., Eur. J. Pharm. Biopharm., 2011, 79(1): 142
4 Purushotham, S., Chang, P.E.J., Rumpel, H., Kee, I.H.C., Ng, R.T.H., Chow, P.K.H., Tan, C.K. and Ramanujan, R.V., Nanotechnology, 2009, 20(30): 305101

5 Davis, M.E., Chen, Z.G. and Shin, D.M., Nat. Rev. Drug Discov., 2008, 7(9): 771
6 Peer, D., Karp, J.M., Hong, S., Farokhzad, O.C., Marglit, R. and Langer, R., Nat. Nanotechnol., 2007, 2(12): 751
7 Hamidi, M., Azadi, A. and Rafiei, P., Adv. Drug. Deliver. Rev., 2008, 60(15): 1638
8 Wu, W., Li, R.T., Bian, X.C., Zhu, Z.S., Ding, D., Li, X.L., Jia, Z.J., Jiang, X.Q. and Hu, Y.Q., ACS Nano, 2009, 3(9): 2740
9 Zhu, Z.S., Xie, C., Liu, Q., Zhen, X., Zheng, X.C., Wu, W., Li, R.T., Ding, Y., Jiang, X.Q. and Liu, B.R., Biomaterials, 2011, 32(35): 9525
10 Petros, R.A. and Desimone, J.M., Nat. Rev. Drug Discov., 2010, 9: 615
11 Aggarwal, P., Hall, J.B., Mcleland, C.B., Dobrovolskaia, M.A. and Mcneil, S.E., Adv. Drug Deliver. Rev., 2009, 61(6): 428
12 Cabral, H., Matsumoto, Y., Mizuno, K., Chen, Q., Murakami, M., Kimura, M., Terada, Y., Kano, M.R., Miyazono, K., Uesaka, M., Nishiyama, N. and Kataoka, K., Nat. Nanotechnol., 2011, 6(12): 815
13 Chen, W.X., Cheng, Y.F. and Wang, B.H., Angew. Chem. Int. Ed., 2012, 51(22): 5293
14 Choi, K.Y., Yoon, H.Y., Kim, J., Bae, S.M., Park, R., Kang, Y.M., Kim, I., Kwon, I.C., Choi, K., Jeong, S.Y., Kim, K. and Park, J.H., ACS Nano, 2011, 5(11): 8591
15 Ellis, G.A., Palte, M.J. and Raines, R.T., J. Am. Chem. Soc., 2012, 134(8): 3631
16 Markovsky, E., Baabur-Cohen, H., Eldar-Boock, A., Omer, L., Tiram, G., Ferber, S., Ofek, P., Polyak, D., Scomparin, A. and Satchi-Fainaro, R., J. Control. Release, 2012, 161(2): 446
17 Werner, M.E., Copp, J.A., Karve, S., Cummings, N.D., Sukumar, R., Li, C., Napier, M.E., Chen, R.C., Cox, A.D. and Wang, A.Z., ACS Nano, 2011, 5(11): 8990
18 Su, J., Chen, F., Cryns, V.L. and Messersmith, P.B., J. Am. Chem. Soc., 2011, 133(31): 11850
19 Li, Y., Xiao, W., Xiao, K., Berti, L., Luo, J., Tseng, H.P., Fung, G. and Lam, K.S., Angew. Chem. Int. Ed., 2012, 51(12): 2864
20 Zaki, N.M., Nasti, A. and Tirelli, N., Macromol. Biosci., 2011, 11(12): 1747
21 Lee, M., Kabilan, S., Hussain, A., Yang, X., Blyth, J. and Lowe, C.R., Anal. Chem., 2004, 76(19): 5748
22 Zhang, L.Z., Lin, Y., Wang, J., Yao, W., Wu, W. and Jiang, X.Q., Macromol. Rapid Commun., 2011, 32(6): 534
23 Kim, D., Gao, Z.G., Lee, E.S. and Bae, Y.H., Mol. Pharm., 2009, 6(5): 1353
24 Behnke, T., Mathejczyk, J.E., Brehm, R., Wurth, C., Gomes, F.R., Dullin, C., Napp, J., Alves, F. and Resch-Genger, U., Biomaterials, 2013, 34(1): 160
25 Kumar, R., Roy, I., Ohulchanskky, T.Y., Vathy, L.A., Bergey, E.J., Sajjad, M. and Prasad, P.N., Acs Nano, 2010, 4(2): 699
26 Souris, J.S., Lee, C., Cheng, S., Chen, C., Yang, C., Ho, J.A., Mou, C. and Lo, L., Biomaterials, 2010, 31(21): 5564
27 Matsymoto, A., Sato, N., Katoka, K. and Miyahara, Y., J. Am. Chem. Soc., 2009, 131(34): 12022
28 Peng, Q., Chen, F., Zhong, Z.L. and Zhuo, R.X., Chem. Commun., 2010, 46(32): 5888
29 Han, H.D., Song, C.K., Park, Y.S., Noh, K.H., Kim, J.H., Hwang, T., Kim, T.W. and Shin, B.C., Int. J. Pharm., 2008, 350(1-2): 27
30 Kratz, F., Ehling, G., Kauffmann, H.M. and Unger, C., Hum. Exp. Toxicol., 2007, 26(1): 19